Rhabdoid Tumor Growth is Inhibited by Flavopiridol

Melissa E. Smith,[1] Velasco Cimica,[1] Srinivasa Chinni,[1] Kavitha Challagulla,[1] Sridhar Mani,[1,2,3] and Ganjam V. Kalpana[1,3]

Abstract

Purpose: Rhabdoid tumors are aggressive and incurable pediatric malignancies. INI1/hSNF5, a tumor suppressor biallelically deleted/inactivated in rhabdoid tumors, directly represses cyclin D1. Rhabdoid tumors and cells are exquisitely dependent on cyclin D1 for genesis and survival, suggesting that targeting the cyclin/cyclin-dependent kinase (cdk) axis may be an effective therapeutic strategy for these tumors. Because cdk inhibitors have not been used for preclinical or clinical testing on rhabdoid tumors, we investigated the effect of flavopiridol, a pan-cdk inhibitor with promising clinical activity, on rhabdoid tumors.

Experimental Design: The effect of flavopiridol on rhabdoid cells was tested *in vitro* using survival, cell cycle, and apoptosis assays. Its effect was assessed *in vivo* using xenografted rhabdoid tumor models. Immunoblot and immunohistochemical analysis was used to assess the effect of flavopiridol on cyclin D1 and p21 expression *in vitro* and *in vivo*, respectively.

Results: Nanomolar concentrations of flavopiridol inhibited rhabdoid cell growth (IC_{50} ~200 nmol/L), induced G_1 and G_2 arrest, and apoptosis *in vitro* in a concentration-dependent manner. These effects were correlated with the down-modulation of cyclin D1, up-regulation of p21, and induction of caspase 3/7 activities. Flavopiridol (at 7.5 mg/kg) significantly inhibited the growth of xenografted rhabdoid tumors, and its effect was correlated with the induction of p21 and down-modulation of cyclin D1.

Conclusions: Flavopiridol is effective in inducing cell cycle arrest and cytotoxicity in rhabdoid tumors. Its effects are correlated with the down-regulation of cyclin D1 and the up-regulation of p21. Flavopiridol is potentially a novel chemotherapeutic agent for rhabdoid tumors.

Rhabdoid tumors are rare but extremely aggressive pediatric malignancies that occur in the kidney (malignant rhabdoid tumors), brain/central nervous system (atypical teratoid and rhabdoid tumors), and soft tissues (extrarenal malignant rhabdoid tumors; ref. 1). Current therapies for rhabdoid tumors involve empirically selected combinations of highly toxic chemotherapeutic agents that are rarely curative (2, 3). Due to the extremely poor prognosis of this disease (15% 2-year survival rate; ref. 1), there is a dire need to develop novel therapies, preferably based on the understanding of the molecular mechanisms underlying the genesis and survival of rhabdoid tumors.

Authors' Affiliations: Departments of [1]Molecular Genetics and [2]Medicine, [3]Albert Einstein College Cancer Center, Bronx, New York

Received 5/31/07; revised 8/27/07; accepted 9/14/07.

Grant support: ACS grant CCG-10493 and the Children's Brain Tumor Foundation, New York (G. Kalpana); Damon Runyon Clinical Investigation grant (S. Mani); and Institutional Training grant NIGMS T32 GM 07491 (M. Smith). G. Kalpana is a Mark Trauner faculty scholar and a recipient of the Irma T. Hirschl Career Scientist Award.

The costs of publication of this article were defrayed in part by the payment of page charges. This article must therefore be hereby marked *advertisement* in accordance with 18 U.S.C. Section 1734 solely to indicate this fact.

Note: M.E. Smith and V. Cimica contributed equally to this work.

Requests for reprints: Ganjam V. Kalpana, Department of Molecular Genetics, Albert Einstein College of Medicine, 1300 Morris Park Avenue, Ullman 821, Bronx, NY 10461. Phone: 718-430-2354; Fax: 718-430-8778; E-mail: kalpana@aecom.yu.edu.

doi:10.1158/1078-0432.CCR-07-1347

Molecular genetic studies have established that rhabdoid tumors are characterized by biallelic deletion/mutation of the *INI1/hSNF5* tumor suppressor (1, 4). INI1 is a component of the SWI/SNF chromatin remodeling complex (5). Reintroduction of INI1 induces G_0-G_1 arrest in rhabdoid cells, directly represses cyclin D1 (6), and activates the cyclin-dependent kinase inhibitors (CDKI), $p16^{INK4a}$ and $p21^{CIP}$ (7). Rhabdoid tumors are dependent on cyclin D1 as shown both *in vitro* and *in vivo*; genetic ablation of cyclin D1 is sufficient to abrogate the formation of rhabdoid tumors in *Ini1*+/- mice (8) and down-modulation of cyclin D1 by RNA interference induces G_0-G_1 arrest and apoptosis in rhabdoid tumor cell lines (9). *Ini1* heterozygous mice develop a high frequency of spontaneous tumors that mimic the etiology, histopathology, and anatomic characteristics of atypical teratoid and rhabdoid tumors and extrarenal rhabdoid tumors (but not renal malignant rhabdoid tumor), as well as overexpress cyclin D1 (6, 8).

Cyclin D1 serves as a key sensor and integrator of extracellular stimuli in the early to mid-G_1 phase of the cell cycle and overcomes the G_1 restriction point (10). Cyclin D1 binds to and activates cyclin-dependent kinases, cdk4 and cdk6, which in turn phosphorylate Rb to inactivate it. Phosphorylation of Rb relieves E2F, activating its target gene transcription. In addition, overexpressed cyclin D1 sequesters $p21^{cip1}$ (cdk inhibitor), activating cyclin E-cdk2 holoenzyme and promoting G_1-S transition. Recent studies using mouse models of breast cancer showed the importance of cdk-dependent functions of cyclin D1 for tumorigenesis (11, 12). Thus, it seems that targeting cdk function may recapitulate the effect of inhibiting

cyclin D1. Because rhabdoid tumors are dependent on cyclin D1, we tested the effectiveness of a pan-cdk inhibitor, flavopiridol, on these tumors.

Flavopiridol is the first broad spectrum cdk inhibitor to enter clinical trails. Recent clinical trials that used pharmacokinetics-derived schedules of flavopiridol administration have shown promising efficacy in inhibiting chronic lymphocytic leukemia (13). Flavopiridol induces cell cycle arrest and apoptosis at low nanomolar concentrations (IC_{50} ~100 nmol/L) *in vitro* (14–17). Flavopiridol is a competitive inhibitor of multiple cdks including cdks 1, 2, 4, 6, 7, and 9 (18). Although its ability to inhibit cdks 1, 2, 4, and 6 directly affects the function of cyclin/cdk complexes resulting in cell cycle arrest, its ability to inhibit cdk9 results in the inactivation of P-TEFb (cyclin T1/cdk9 complex), blocking RNA polymerase II–mediated transcription of many genes including cyclin D1 (18–20). Flavopiridol also affects cyclin D1 through its ability to indirectly inhibit tumor necrosis factor–induced nuclear factor-κB (17), and inhibits the activation of Akt, which leads to decreased cyclin D1 translation (21). Thus, it seems that flavopiridol is able to inhibit cyclin and cdk protein and activity levels through multiple mechanisms. Due to flavopiridol's effect on various aspects of the cyclin/cdk axis, we tested its ability to inhibit the growth of rhabdoid cells *in vitro* and of xenografted rhabdoid tumors *in vivo*. Our results, presented here for the first time, indicate that flavopiridol has strong inhibitory effects on the growth of rhabdoid cells and tumors, and that its effects are correlated with the down-modulation of cyclin D1.

Materials and Methods

Cell culture and drugs. The rhabdoid tumor cell lines (*INI1*-/-) used, MON (4) and G401 (American Type Culture Collection) were maintained in RPMI supplemented with 10% fetal bovine serum. Twenty-four hours before plating cells for drug treatment, cultures were transferred to RPMI supplemented with 10% bovine serum pretreated with charcoal and dextran (HyClone). Flavopiridol was obtained through the Cancer Therapy Evaluation Program at National Cancer Institute (courtesy of Dr. Colevas) and the pan-caspase inhibitor, z-VAD-FMK, was purchased from Promega. Flavopiridol stock solution at 10 mmol/L concentration was prepared in DMSO. The working solution (3 μmol/L) and serial dilutions were prepared by diluting the stock solution with culture medium, such that the final concentration of DMSO was 0.03% in all the dilutions.

Analysis of drug effects on cell proliferation (MTS assay). Aliquots of 8×10^3 cells were plated in 96-well plates and treated with serial dilutions of flavopiridol for 1, 2, or 5 days. Cell survival was determined using an MTS assay kit (CellTiter 96 Aqueous One Solution Cell Proliferation Assay Kit; Promega). Cell plating, drug treatment, and survival assay were done using the epMotion 5070 automated liquid handling system (Eppendorff).

Cell cycle and apoptosis analysis. Propidium iodide staining and fluorescence activated cell sorting (FACS) analysis was done as described previously (6). Data was elaborated using CellQuest Pro software (BD Biosciences). Apoptosis was assessed by gating for a sub-G_1 population during FACS and by caspase 3/7 activation using the Caspase-Glo 3/7 Assay Kit (Promega), as previously described (9).

Statistical analysis. Data was analyzed as previously described (9) using GraphPad Prism (GraphPad Software) to evaluate the numbers for each data group (e.g., controls and flavopiridol-treated) and one-way ANOVA or *t* test was used.

Immunoblot analysis. Immunoblot analysis was carried out as described previously (6). The following antibodies were used: cyclin D1 (Lab Vision), cdk2 (Santa Cruz), cdk4 (Santa Cruz), p21 (Calbiochem), and glyceraldehyde-3-phosphate dehydrogenase (Chemicon). Chemiluminescence detection was achieved using SuperSignal West Pico Chemiluminescence Substrate (Pierce).

Testing the effect of flavopiridol on xenografted rhabdoid tumors in vivo. As described previously, xenografts were generated by s.c. inoculating ~10^7 rhabdoid cells into the right flank of nude, severe combined immunodeficiency (SCID), SCID-Beige, and ICR-SCID mice purchased from Taconic. Tumors were measured twice a week manually, using a digital Vernier caliper, and tumor volumes were calculated using the formula $0.5 \times l \times h \times w$. For the assessment of flavopiridol's effect, SCID mice injected with G401 cells were used (9). After the tumors were implanted and reached a palpable size (average tumor volume of ~45 mm^3), the mice were randomized into control and treatment groups (n = 8-10). Control mice received vehicle (0.1% DMSO in saline) and treated mice received 2.5, 5.0, or 7.5 mg/kg of flavopiridol intraperitonially (i.p.), 5 days a week for either 3 weeks (for mice that received 2.5 and 5.0 mg/kg) or 2 weeks (for mice that received 7.5 mg/kg). For xenograft studies, weekly doses of 1 mg/mL of the flavopiridol solution was prepared in 0.9% saline (AmTech) containing 0.1% DMSO, heated to 37°C and subjected to vigorous vortexing to dissolve the clumps, and stored frozen at -80°C. At the time of treatment, the solution was gently heated to 37°C and vortexed before injection. The growth of tumors was monitored as before, by using a Vernier caliper (9). The percentage of tumor volume was calculated by considering the starting tumor volume of the day of drug injection as 100%.

Immunohistochemical analysis. Staining was done using antibodies: p21 (Calbiochem), cyclin D1 (Cell Marque). Tumor xenografts were removed, washed in PBS, fixed in 4% buffered formalin solution overnight, and embedded in paraffin blocks. Sections of 6 to 7 μm were deparaffinized in xylene and hydrated with graded alcohols and distilled water. Antigen retrieval was achieved by boiling the slides in a microwave for 10 to 20 min in EDTA (for cyclin D1), or citrate (for p21) buffers. Endogenous peroxidase was quenched using 0.3% hydrogen peroxide solution. Slides were incubated with primary antibody overnight at 4°C. Secondary antibody was incubated for 30 min at room temperature. The antigen-antibody reaction was visualized using the 3,3′-diaminobenzidine system (SIGMA) and Envision Kit (DAKO). Sections were counterstained with hematoxylin (Vector Laboratories) cleared in alcohol and xylene and mounted with Histomount (Zymed; ref. 9).

Results

Low nanomolar concentrations of flavopiridol effectively inhibit rhabdoid cell growth. We used an MTS assay to analyze the effect of flavopiridol on the survival of MON and G401, two *INI1*-/- human rhabdoid tumor cell lines. Treatment of cells with flavopiridol for 1, 2. and 5 days resulted in a dose-dependent decrease in cell proliferation with IC_{50}'s ranging from 150 to 200 nmol/L in both cell types (Fig. 1A and B). Although the IC_{50} values were similar for different exposure periods (1, 2, or 5 days), maximal cell killing was dramatically increased at drug concentrations of ≥400 nmol/L in a time-dependent manner. Specifically, at concentrations of ~100 nmol/L of flavopiridol, the percentage of cell killing remained ~20% with different days of exposure of the cells to flavopiridol (Fig. 1C and D). However, at 400 nmol/L or higher concentrations, increasing time of exposure to drug dramatically increased the percentage of cell killing, reaching 95% to 100% cell death after 5 days of treatment ($P < 0.0001$ for both MON and G401 cells; Fig. 1C and D). These results indicate that increasing the time of exposure to flavopiridol increases cell killing at concentrations of ≥400 nmol/L.

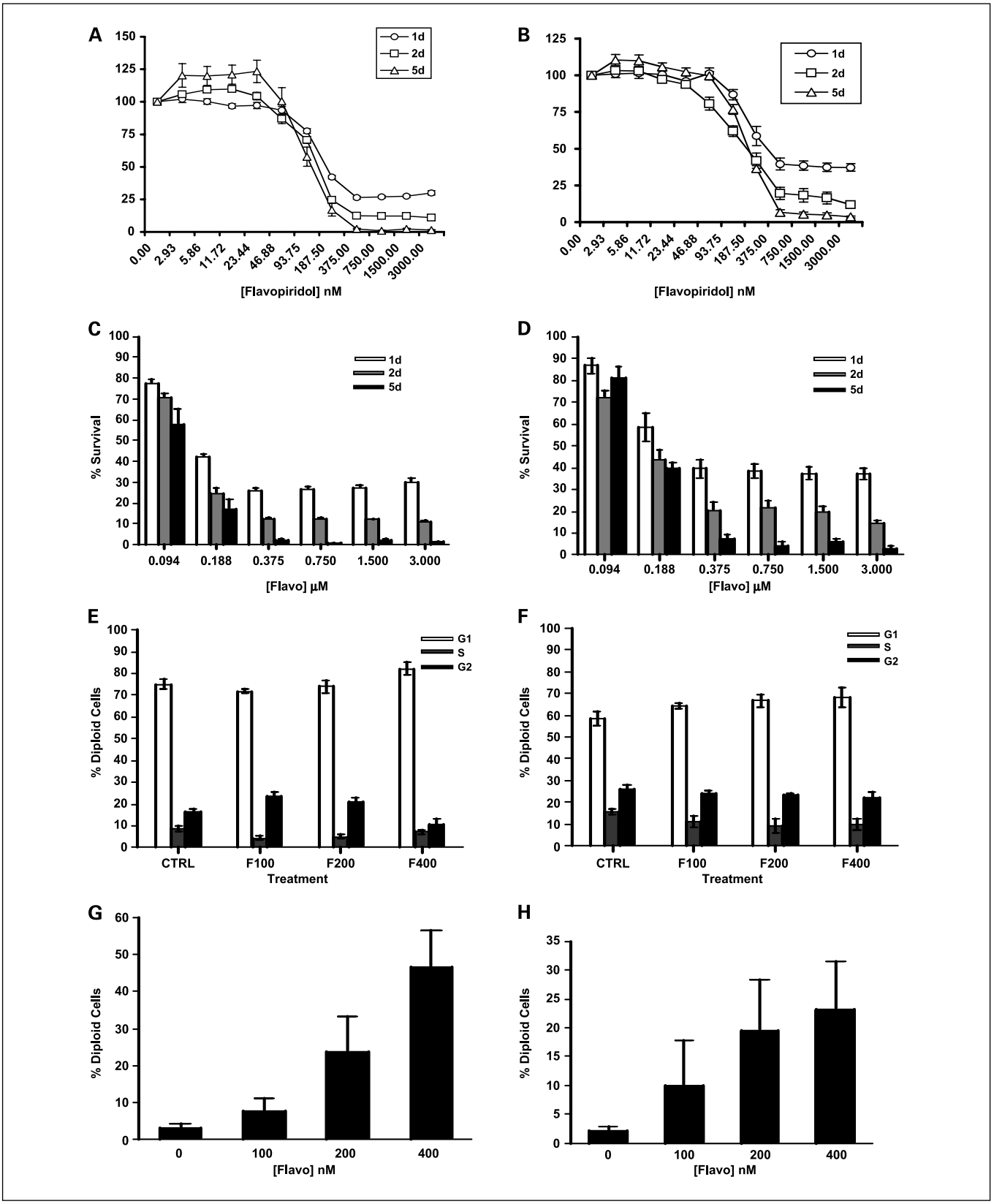

Fig. 1. Flavopiridol inhibits rhabdoid cell survival and induces cell cycle arrest and apoptosis. *A* and *B,* survival curves of MON (*A*) and G401 (*B*) cells treated with increasing concentrations of flavopiridol for 1, 2, and 5 d and subjected to MTS assay. *C* and *D,* graphical representation to indicate time of exposure-dependent increase of flavopiridol-mediated cytotoxicity in MON (*C*) and G401 (*D*) cells. The values were derived from (*A* and *B*). *E* and *F,* cell cycle profile of diploid cell population determined by FACS analysis of MON (*E*) and G401 (*F*) cells treated with the indicated concentrations of flavopiridol for 48 h. *G* and *H,* percentage of MON (*G*) and G401 (*H*) cells at sub-G_1 when exposed to flavopiridol for 48 h.

Flavopiridol induces cell cycle arrest and apoptosis in rhabdoid cells. To determine the mechanism of flavopiridol-induced effect on survival, cells were exposed to 100, 200, and 400 nmol/L of the drug for 2 days and subjected to FACS analysis. The results indicated that flavopiridol induced G_2 arrest at 100 nmol/L ($P = 0.05$) and G_1 arrest at 400 nmol/L ($P = 0.039$) in MON cells and specifically induced G_1 arrest in G401 cells ($P = 0.047$ at 200 nmol/L and $P = 0.049$ at 400 nmol/L; Fig. 1E and F). Furthermore, analysis of the sub-G_1 fraction of cells indicated that flavopiridol induced a dose-dependent increase in cell death in both cell types (Fig. 1G and H).

Mechanism of cell death and cell cycle arrest induced by flavopiridol. Flavopiridol induces cell death by both caspase-dependent and -independent mechanisms (21). To determine the mechanism of flavopiridol-induced cell death in rhabdoid cells, MON and G401 cells were treated with increasing concentrations of the drug for 2 days in the presence and absence of a pan-caspase inhibitor, z-VAD-FMK. FACS analysis was then carried out to determine the percentage of sub-G_1 cells. The addition of a caspase inhibitor had no significant effect on the cell cycle profile (data not shown), but dramatically decreased the percentage of sub-G_1 cells at all concentrations of the drug used, indicating that flavopiridol-induced cell death is caspase-dependent ($P = 0.0079$ for MON and 0.0028 for G401; Fig. 2A and B).

To determine if caspase 3/7 activities are induced upon flavopiridol treatment, cells were exposed to increasing concentrations of flavopiridol for various time points and subjected to the Caspase-Glo assay. The results of this analysis indicated that flavopiridol induced caspase 3/7 activity in MON and G401 cells in a dose- and time-dependent manner with activities observed at ~12 h posttreatment ($P < 0.0001$; Fig. 2C and D). These results indicate that flavopiridol induces caspase 3/7–mediated apoptosis in rhabdoid cells.

To determine the effect of flavopiridol on cell cycle regulators, we carried out immunoblot analyses of proteins isolated from MON and G401 cells treated for 2 days with different concentrations of flavopiridol. At 100 nmol/L, flavopiridol increased p21 levels in both MON and G401 cells (Fig. 2E). At 200 nmol/L, flavopiridol dramatically induced p21, and furthermore, led to a drastic decrease in cyclin D1 (Fig. 2E). Interestingly, 400 nmol/L of flavopiridol down-modulated both cyclin D1 and p21 levels. These results are intriguing and correlated with the effect of the drug on cell growth and cell cycle arrest. In particular, down-regulation of both cyclin D1 and p21 at 400 nmol/L of flavopiridol was consistent with the dramatic cell-killing effects seen at this concentration (Fig. 1A-D). These results indicate that flavopiridol induces cell cycle arrest and cytotoxicity by down-modulating cyclin D1, altering p21 levels, and up-regulating caspase 3/7 activities in rhabdoid cells.

Development of xenograft mouse models of rhabdoid tumors. Previously, we have been successful in generating xenografts of rhabdoid tumors by inoculating G401 cells s.c. in SCID mice (9). To test the generation of xenografts with MON cells, we inoculated these cells into SCID mice and found that no xenografts were implanted to form tumors (data not shown). These results prompted us to investigate the generation of xenografts from three commonly used rhabdoid cell lines (MON, G401, and STA-WT1) using various mouse strains. We used mice from four different genetic backgrounds including athymic nude, SCID, SCID-BEIGE, and ICR-SCID mice. The nude mice are T cell–deficient, but have normal B cell and natural killer cell functions (22). SCID mice are deficient for both T cells and B cells due to a defect in V(D)J recombination, however, have a leakiness in the expression of immunoglobulins and therefore exhibit low levels of immunoglobulins in ~20% of mice beginning at 12 weeks of age (23, 24). ICR-SCID mice are similar to SCID mice, except that they exhibit a significantly reduced incidence of spontaneous immunoglobulin production (23, 24). SCID-BEIGE mice are deficient for both B cells and T cells due to a defect in V(D)J recombination, as well as the presence of a Beige mutation that causes the impairment of cytotoxic T cells, macrophages, and selective natural killer cell functions (25).

Three different rhabdoid cell lines were inoculated into these four mouse strains, and tumor implantation and growth were monitored by measuring the tumor volume periodically. The growth characteristics of rhabdoid cells in different strains of mice varied significantly. MON cells implanted only in nude mice, in which they reached a maximum tumor volume of ~100 mm^3 and subsequently ceased to grow (Fig. 3A). Analysis of dissected xenografted tumors from these mice indicated the presence of a large degree of necrosis and fibrosis (data not shown). Other cell lines (G401, STA-WT1) although implanted efficiently in all four strains of mice, exhibited variability in terms of rate of growth, consistency, and interindividual variability (Fig. 3B-I). We observed that G401 cells, when inoculated into SCID mice, showed the most favorable growth pattern, exhibiting the least interindividual variability and a uniform tumor growth upon implantation (Fig. 3G). Thus, we chose xenografts derived from G401 cells inoculated into SCID mice to test the effect of flavopiridol *in vivo*.

Flavopiridol is effective in inhibiting xenografted rhabdoid tumors. To determine the effect of flavopiridol *in vivo*, G401 cells were inoculated into SCID mice. When the tumors were established and reached an average volume of ~45 mm^3, the mice were randomized into control and treatment groups. Mice in the control group received vehicle, whereas those in the treatment groups received 2.5 or 5.0 mg/kg of flavopiridol 5 days a week for 3 weeks. This was followed by an observation period of 3 to 4 weeks without drug treatment. Flavopiridol at 2.5 and 5.0 mg/kg had a minimal effect on xenografted tumor growth (Fig. 4A). Therefore, we treated another cohort of mice with 7.5 mg/kg of flavopiridol 5 days a week for 2 weeks and observed them for an additional 2 weeks without treatment. Flavopiridol at 7.5 mg/kg significantly inhibited xenograft tumor growth resulting in a reduction of average tumor volume compared with the controls ($P = 0.0096$; Fig. 4B). Analysis of tumor weights at the end of the treatment period indicated a significant decrease in average tumor weights consistent with the decrease in average tumor volume ($P = 0.039$; Fig. 4C). We found that flavopiridol treatment resulted in a slight weight loss in mice during the treatment period. However, these mice regained any lost weight during the posttreatment observation period (data not shown). These results indicate that 7.5 mg/kg of flavopiridol is effective in inhibiting xenografted rhabdoid tumor growth.

Flavopiridol treatment decreases cyclin D1- and increases p21-positive cells in rhabdoid tumor xenografts. Immunoblot analysis of rhabdoid tumor cells *in vitro* showed that the levels

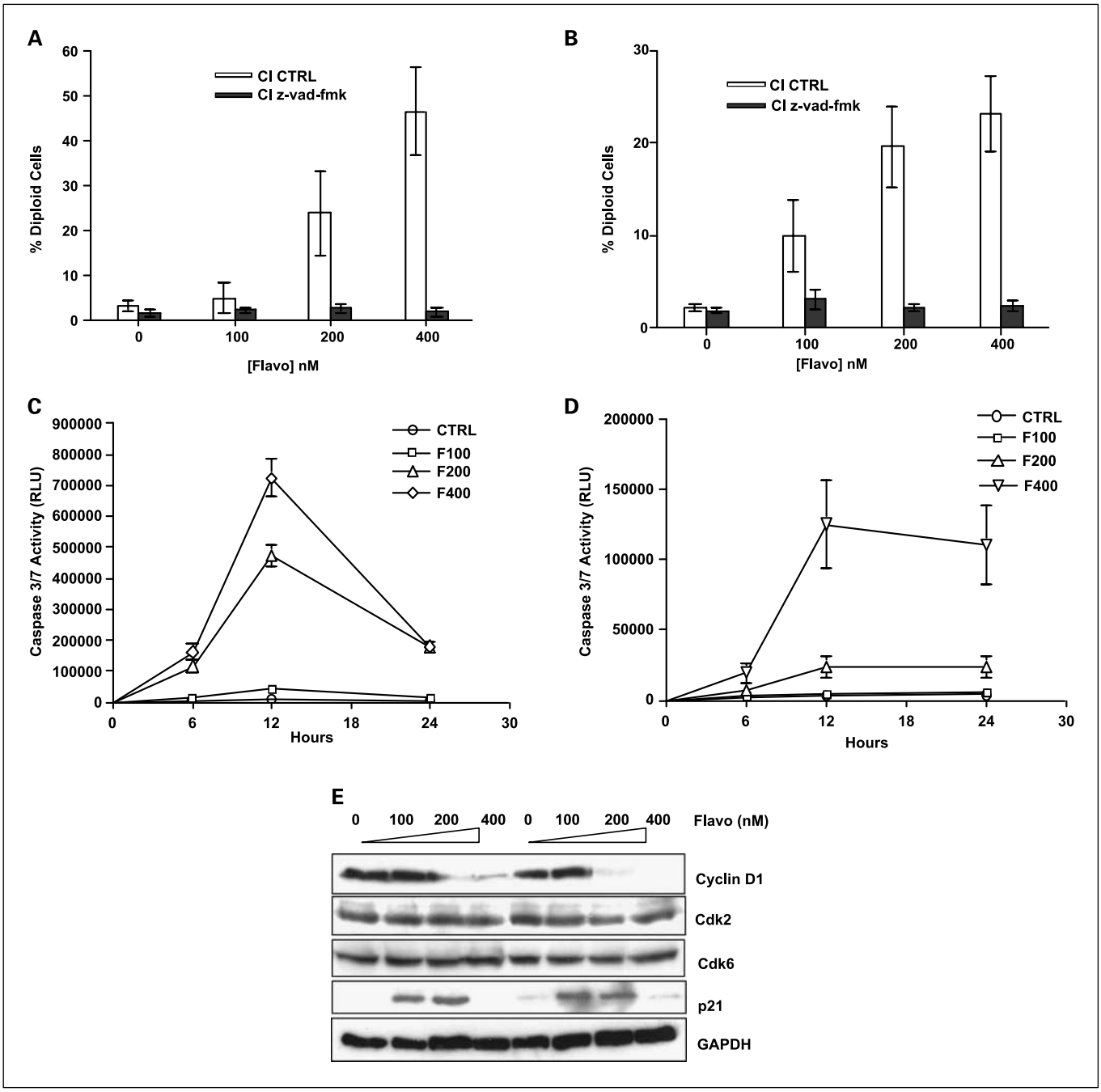

Fig. 2. Mechanism by which flavopiridol induces cell cycle arrest and apoptosis in rhabdoid tumor cells. *A* and *B,* percentage of MON (*A*) and G401 (*B*) cells at sub-G_1 when treated for 48 h with flavopiridol in the presence of a pan-caspase inhibitor, z-VAD-FMK (*CTRL,* control not treated with caspase inhibitor; *CI,* caspase inhibitor). *C* and *D,* kinetics of caspase 3/7 activation in MON (*C*) and G401 (*D*) cells treated with the indicated concentrations of flavopiridol (in nmol/L; *F,* flavopiridol; *CTRL,* control vehicle). *E,* immunoblot analysis of various cell cycle proteins after 48 h of treatment with the indicated concentrations of flavopiridol.

of cyclin D1 and p21 are modulated by different concentrations of flavopiridol (Fig. 2E). To determine if flavopiridol-mediated reduction of tumor growth correlated with the regulation of cyclin D1 and p21 *in vivo*, tumors from three control and three flavopiridol-treated mice were analyzed for the expression of these two proteins by immunohistochemical analysis, at the termination of the experiment. The results indicated that although untreated control xenograft tumors exhibited pockets of strong nuclear staining of cyclin D1 (Fig. 5, 1-3), there was a significant reduction in intensity and percentage of cells positive for cyclin D1 in treated tumors (Fig. 5, 4-6). Interestingly, the ratio of nonneoplastic stromal cells to neoplastic cells greatly increased in flavopiridol-treated tumors, as compared with that of the control tumors (Fig. 5, compare 1-3 to 4-6).

Flavopiridol-treated tumors exhibited an increase in the number of cells positive for p21 when compared with that of the controls (Fig. 5, compare 7-9 to 10-12). Positive staining for

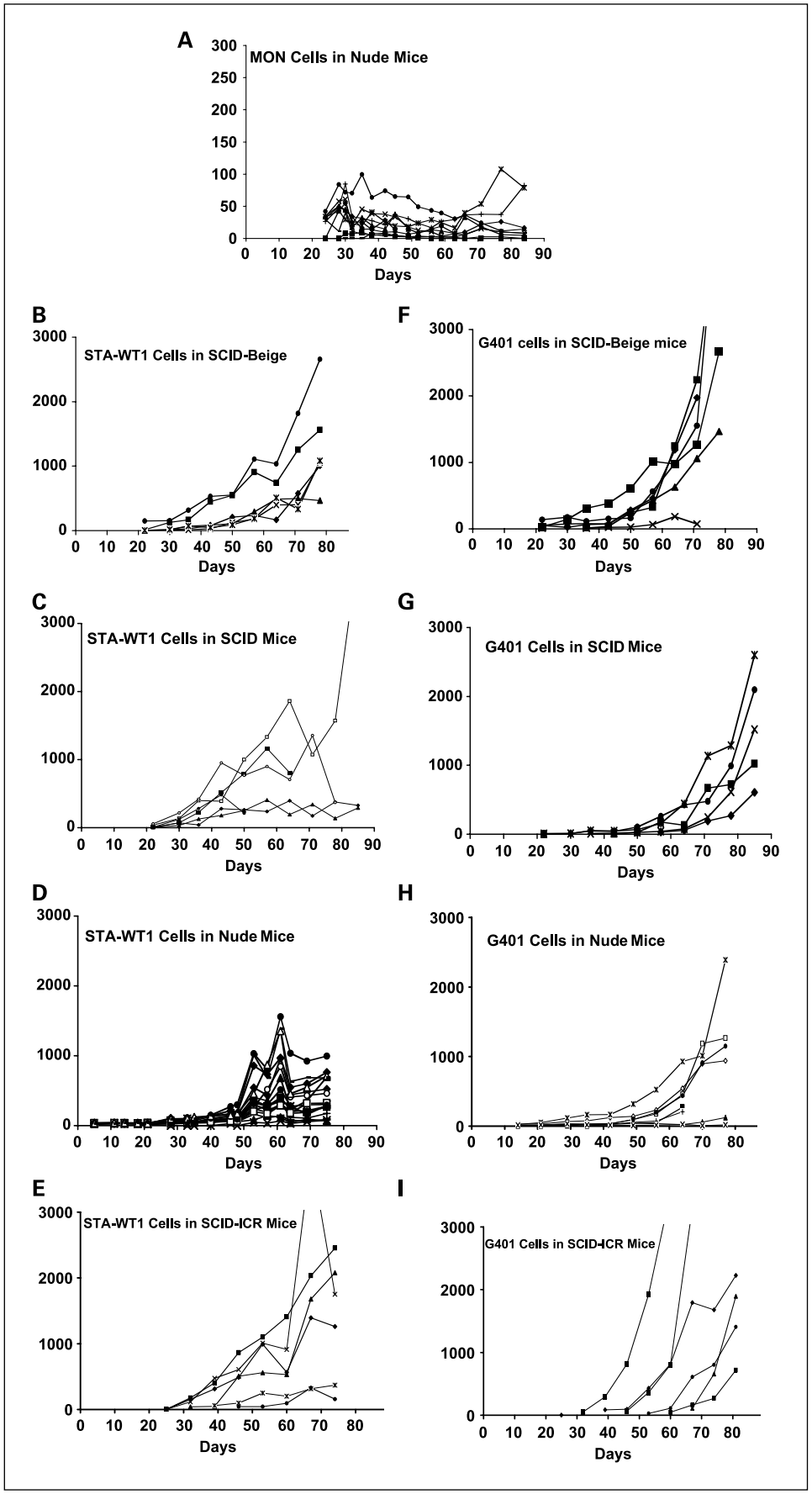

Fig. 3. Comparative analysis of rhabdoid tumor xenograft growth using different rhabdoid cell lines and mouse strains. *A,* growth of MON cells as xenograft tumors when injected into nude mice; *B-E,* growth of STA-WT1 cells injected into SCID beige (*B*), SCID (*C*), nude (*D*), and ICR-SCID (*E*) mice; *F-I,* growth of G401 cells injected into SCID beige (*F*), SCID (*G*), nude (*H*), and ICR-SCID (*I*) mice. Please note different *Y*-axis scale for (*A*), in which MON cells inoculated into nude mice exhibited an inefficient growth pattern. *Y*-axes indicate tumor volume.

p21 was selectively observed in neoplastic cells of the treated tumors, whereas the stromal cells were largely negative (Fig. 5, 10-12). Together, these results indicate that the inhibitory effect of flavopiridol on xenografted tumors was correlated to a decrease in cyclin D1–positive cells and an increase in p21-positive cells.

Discussion

Rhabdoid tumors are highly aggressive and incurable pediatric malignancies. Despite a lack of standard or effective therapy for rhabdoid tumors, molecular biology of these tumors is well characterized (1). Understanding the detailed molecular mechanisms of rhabdoid tumorigenesis should pave the way to developing molecularly targeted therapies for rhabdoid tumors. Based on studies that have shown the essential role of cyclin D1 for rhabdoid tumorigenesis, we surmised that targeting the cyclin/cdk axis could be effective in inhibiting rhabdoid tumor growth (8, 9). Here, we report that the use of a pan-cdk inhibitor, flavopiridol, that both inhibits cdk activity and transcriptionally down-modulates cyclin D1, effectively inhibits rhabdoid tumor growth.

Our results indicate that low nanomolar concentrations of flavopiridol (IC_{50}, 150-200 nmol/L) have strong growth-inhibitory effects on rhabdoid cell lines *in vitro*. We found that increasing the time of exposure to flavopiridol *in vitro* did not change the IC_{50} values, but dramatically increased cytotoxicity at concentrations >400 nmol/L (Fig. 1C and D). The exact reason for this increased cytotoxicity is unclear at this point. However, it is interesting to note that flavopiridol inhibited both cyclin D1 and p21 at 400 nmol/L concentrations (Fig. 2E). At lower concentrations (100-200 nmol/L), flavopiridol did not inhibit cyclin D1. It is therefore possible that increased cytotoxicity is related to the down-modulation of cyclin D1, as we found that inhibiting cyclin D1 in rhabdoid cells induces apoptosis in addition to G_1 arrest (9). Understanding the mechanistic basis of increased cytotoxicity of flavopiridol is valuable for improving its clinical efficacy.

Flavopiridol induced cell cycle arrest in a concentration- and cell type–dependent manner; whereas only MON cells exhibited G_2 arrest at 100 nmol/L of flavopiridol, both MON and G401 cells exhibited G_1 arrest at 400 nmol/L concentrations of flavopiridol (Fig. 1E). Flavopiridol differentially affected cyclin D1 and p21 levels—100 nmol/L of flavopiridol increased p21 and had no effect on cyclin D1; 200 nmol/L of flavopiridol moderately inhibited cyclin D1 and induced p21; and 400 nmol/L of flavopiridol reduced both cyclin D1 and p21 (Fig. 2E). We believe that concentration-dependent variability in biomarker expression and its correlation to flavopiridol-induced cytotoxicity *in vitro* may provide necessary insight to correlate its effect *in vivo*. For example, clinically achievable concentrations of flavopiridol are variable depending on the route, mode of administration, and other biological variables, which in turn, results in variability in the efficacy and in biomarker expression. This is reflected in the fact that although some reports correlate the up-regulation of p21 expression with the effect of flavopiridol (26–28), other reports correlate the down-regulation of p21 with the effects of flavopiridol (29–33). Our studies indicate that the differences in the biomarker expression could reflect the drug concentration achieved within tumors (also see below).

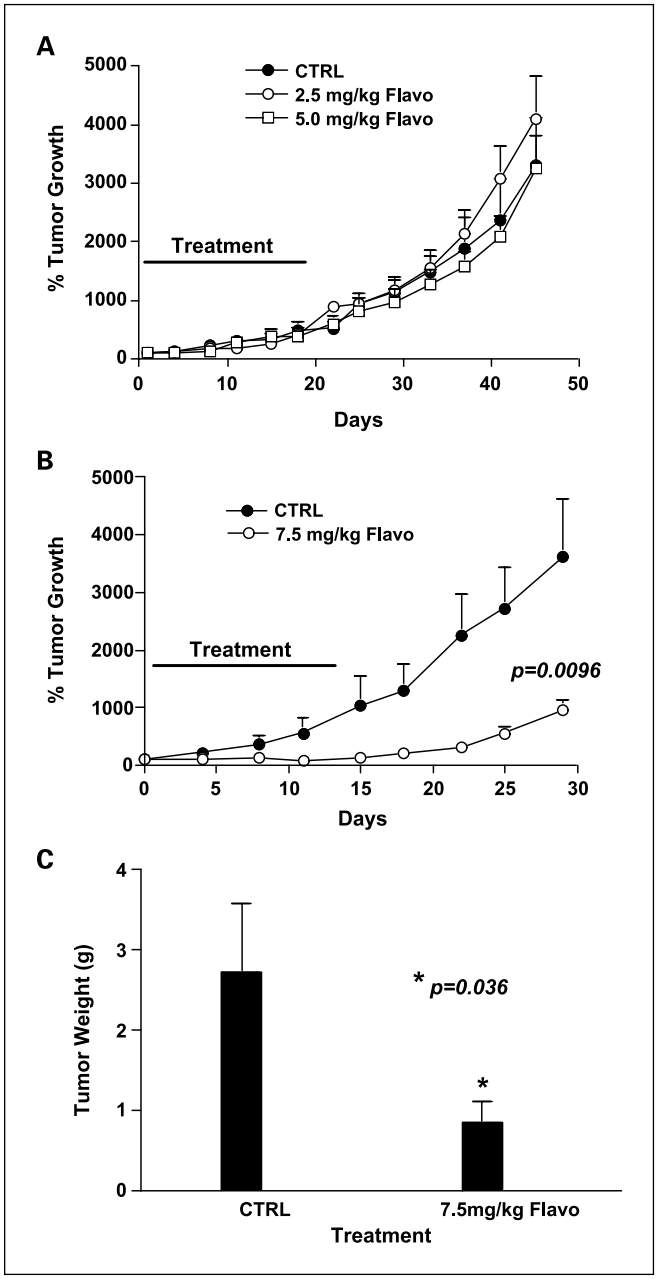

Fig. 4. Effect of flavopiridol on xenografted tumors. *A,* mice bearing established xenografts were treated with vehicle control or flavopiridol at 2.5 or 5.0 kg/kg for 5 d each for 3 wk. The growth of tumors was monitored by measuring tumor volume. The graphs indicate the percentage of tumor growth in control and flavopiridol-treated groups. *B,* xenograft tumors were established as in (*A*), and the mice were treated with control vehicle or 7.5 mg/kg of flavopiridol, 5 d per week for 2 wk. *C,* average tumor weights at the termination of the protocol in control and 7.5 mg/kg of flavopiridol-treated groups.

Our attempt to develop a xenograft model for rhabdoid tumors showed the variability with which rhabdoid cells implant in mouse strains with differing genetic backgrounds. It is intriguing to note that nude mice were less suitable for xenograft tumor formation when human rhabdoid tumor cell lines were used (Fig. 3). Previous studies have reported the use of nude mice for explants of human rhabdoid tumors (34, 35), indicating that the observed results are likely to represent a cell line–dependent phenomenon. Our studies indicate that it is

possible to increase the efficiency of rhabdoid tumor implantation and growth based on the mouse strain, and that it might be possible to inhibit tumor growth by immunologic means.

Our results, for the first time, indicate that 7.5 mg/kg of flavopiridol is effective in significantly decreasing the growth of pre-established xenograft tumors. Analysis of biomarker expression in xenografts indicated that whereas cyclin D1 was down-regulated, p21 was up-regulated by flavopiridol treatment. Because the expression of cyclin D1 and p21 varied depending on the flavopiridol concentration *in vitro*, we surmise that we have been able to achieve only intermediate concentrations of flavopiridol (~200 nmol/L) in the xenograft tumors. Improving means to increase the concentration of drug within the tumor (≥400 nmol/L) is likely to further increase drug efficacy, which could then be monitored by the analysis of the two biomarkers, cyclin D1 and p21.

The drug concentrations and schedule of flavopiridol used in this study are based on previous preclinical reports (36). It was

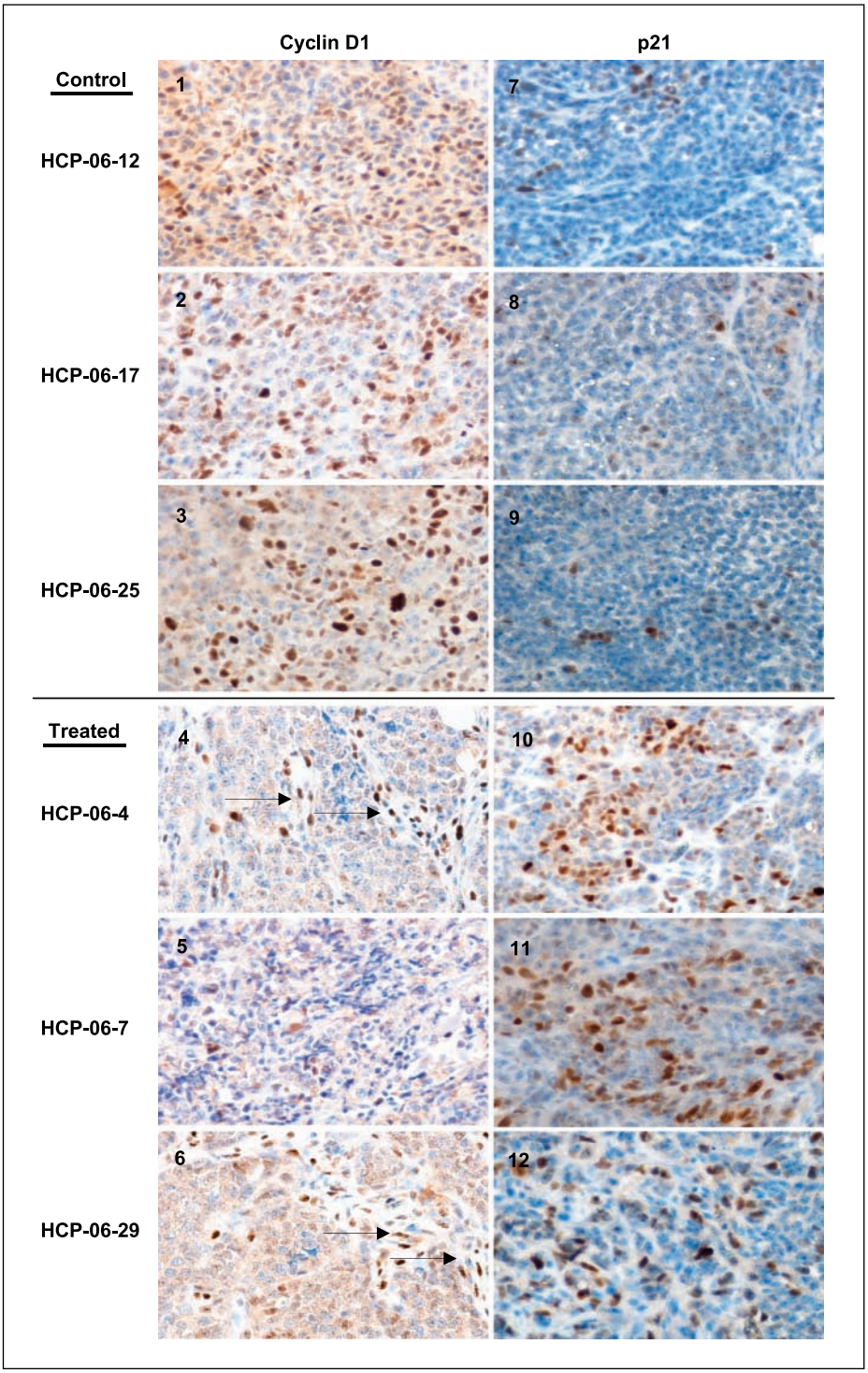

Fig. 5. Immunohistochemical analysis of xenograft tumors. Three control (HCP-06-12, -17, and 25) and three treated tumors and HCP-06-4, -7, and -29 were stained for cyclin D1 (*1-6*) and p21 (*7-12*). Cyclin D1, but not p21, staining was noted in nonneoplastic stromal cells (*black arrows, 4-6*). Note the decrease of cyclin D1 – positive neoplastic cells and the increase of p21-positive cells in flavopiridol-treated tumors.

reported that after daily (i.p. or i.v.) injections of 5 mg/kg of flavopiridol for 1 to 5 days, the plasma concentrations reached a maximum of ~7 μmol/L and declined in a biexponential manner to 0.1 μmol/L after 8 h (36). Furthermore, it was shown that after daily treatments with 7.5 mg/kg of flavopiridol by an i.p. or i.v. bolus for 5 consecutive days, 11 out of 12 advanced stage subcutaneous human HL60 xenografts underwent complete regression (36). Phase I clinical studies of flavopiridol have shown that peak concentrations and the area under the curve of flavopiridol were linear at various doses (37). Furthermore, the area under the curve and clearance were comparable between the 1-h infusion and 72-h CIV (continous infusion) schedule and the area under the curve in mice at a dose of 5 mg/kg/d for 5 days was comparable with the area under the curve of flavopiridol administered over 1 h at the dose of 37.5 mg/m^2/d for 5 days (Stinson, unpublished results in ref. 37). Assuming that pharmacokinetics is dose-proportional in mice (as it is in humans; ref. 37), then a 7.5 mg/kg dose in mice would be similar to a 56.25 mg/m^2/d dose in humans (7.5/5 × 37.5 mg/kg). Phase I trials of flavopiridol in children have indicated that toxicity profile, pharmacokinetics, and maximum tolerable dose were similar to that in adults (38). Furthermore, it was shown that the maximum tolerable dose of flavopiridol in children was 62.5 mg/m^2/d (without prophylaxis) and 80 mg/m^2/d (with prophylaxis) when administered for 3 days (38), indicating that the use of flavopiridol in rhabdoid patients, a largely pediatric population, is feasible.

Flavopiridol has shown efficacy in clinical trials of chronic lymphocytic leukemia, in which a pharmacokinetics-derived schedule of administration were used (13). The schedule involved a 30-min loading dose, followed by 4 h of infusion administered weekly for 4 to 6 weeks. Using these novel clinical protocols, a long-term high-plasma concentration of flavopiridol (~1.5 μmol/L), could be achieved, which is above the concentration of the drug required to inhibit the tumor growth as indicated in preclinical models. These studies suggest that the concentration of flavopiridol required to inhibit rhabdoid tumor growth could be clinically achieved.

The aggressive and incurable nature of rhabdoid tumors corroborates the need to develop a targeted and effective therapy for these tumors. Our results indicate that targeting the cyclin/cdk axis is a novel and effective approach in achieving this goal. Our previous studies using fenretinide showed efficacy in inhibiting rhabdoid tumor growth in correlation with the inhibition of cyclin D1 (9). In this report, we show, for the first time, that the pan-cdk inhibitor flavopiridol is effective in inhibiting rhabdoid tumor growth *in vitro* and *in vivo*. These findings strengthen our hypothesis that targeting the cyclin/cdk axis is an effective means of therapy against rhabdoid tumors. We therefore propose that flavopiridol should be tested in children with rhabdoid tumors in which there is a dire need for an effective therapy.

Acknowledgments

We thank Drs. Goldman and Prasad at AECOM for useful discussions, Dr. Colevas at the Cancer Therapy Evaluation Program, National Cancer Institute for providing flavopiridol, and Dr. Zhikai Zhang for initiating the flavopiridol project on rhabdoid cell lines in the laboratory.

References

1. Biegel JA. Molecular genetics of atypical teratoid/rhabdoid tumor. Neurosurg Focus 2006;20:E11.
2. Packer RJ, Biegel JA, Blaney S, et al. Atypical teratoid/rhabdoid tumor of the central nervous system: report on workshop. J Pediatr Hematol Oncol 2002;24:337–42.
3. Strother D. Atypical teratoid rhabdoid tumors of childhood: diagnosis, treatment and challenges. Expert Rev Anticancer Ther 2005;5:907–15.
4. Versteege I, Sévenet N, Lange J, et al. Truncating mutations of hSNF5/INI1 in aggressive paediatric cancer. Nature 1998;394:203–6.
5. Wang W, Cote J, Xue Y, et al. Purification and biochemical heterogeneity of the mammalian SWI-SNF complex. EMBO J 1996;15:5370–82.
6. Zhang ZK, Davies KP, Allen J, et al. Cell cycle arrest and repression of cyclin D1 transcription by INI1/hSNF5. Mol Cell Biol 2002;22:5975–88.
7. Chai J, Charboneau AL, Betz BL, Weissman BE. Loss of the hSNF5 gene concomitantly inactivates p21CIP/WAF1 and p16INK4a activity associated with replicative senescence in A204 rhabdoid tumor cells. Cancer Res 2005;65:10192–8.
8. Tsikitis M, Zhang Z, Edelman W, Zagzag D, Kalpana GV. Genetic ablation of cyclin D1 abrogates rhabdoid tumours arising due to Ini1 loss. Proc Natl Acad Sci U S A 2005;102:12129–34.
9. Alarcon-Vargas D, Zhang Z, Agarwal B, Challagulla K, Mani S, Kalpana GV. Targeting cyclin D1, a downstream effector of INI1/hSNF5, in rhabdoid tumors. Oncogene 2006;25:722–34.
10. Ewen ME, Lamb J. The activities of cyclin D1 that drive tumorigenesis. Trends Mol Med 2004;10:158–62.
11. Yu Q, Sicinska E, Geng Y, et al. Requirement for CDK4 kinase function in breast cancer. Cancer Cell 2006;9:23–32.
12. Landis MW, Pawlyk BS, Li T, Sicinski P, Hinds PW. Cyclin D1-dependent kinase activity in murine development and mammary tumorigenesis. Cancer Cell 2006;9:13–22.
13. Byrd JC, Lin TS, Dalton JT, et al. Flavopiridol administered using a pharmacologically derived schedule is associated with marked clinical efficacy in refractory, genetically high-risk chronic lymphocytic leukemia. Blood 2007;109:399–404.
14. Kelland LR. Flavopiridol, the first cyclin-dependent kinase inhibitor to enter the clinic: current status. Expert Opin Investig Drugs 2000;9:2903–11.
15. Senderowicz AM. Cyclin-dependent kinases as targets for cancer therapy. Cancer Chemother Biol Response Modif 2002;20:169–96.
16. Tan AR, Swain SM. Review of flavopiridol, a cyclin-dependent kinase inhibitor, as breast cancer therapy. Semin Oncol 2002;29:77–85.
17. Takada Y, Aggarwal BB. Flavopiridol inhibits NF-κB activation induced by various carcinogens and inflammatory agents through inhibition of IκBα kinase and p65 phosphorylation: abrogation of cyclin D1, cyclooxygenase-2, and matrix metalloprotease-9. J Biol Chem 2004;279:4750–9.
18. Chao SH, Price DH. Flavopiridol inactivates P-TEFb and blocks most RNA polymerase II transcription *in vivo*. J Biol Chem 2001;276:31793–9.
19. de Azevedo WF, Jr., Canduri F, da Silveira NJ. Structural basis for inhibition of cyclin-dependent kinase 9 by flavopiridol. Biochem Biophys Res Commun 2002;293:566–71.
20. Mani S, Wang C, Wu K, Francis R, Pestell R. Cyclin-dependent kinase inhibitors: novel anticancer agents. Expert Opin Investig Drugs 2000;9:1849–70.
21. Newcomb EW. Flavopiridol: pleiotropic biological effects enhance its anti-cancer activity. Anticancer Drugs 2004;15:411–9.
22. Pantelouris EM. Absence of thymus in a mouse mutant. Nature 1968;217:370–1.
23. Bosma MJ. B and T cell leakiness in the scid mouse mutant. Immunodefic Rev 1992;3:261–76.
24. Bosma MJ, Carroll AM. The SCID mouse mutant: definition, characterization, and potential uses. Annu Rev Immunol 1991;9:323–50.
25. MacDougall JR, Croy BA, Chapeau C, Clark DA. Demonstration of a splenic cytotoxic effector cell in mice of genotype SCID/SCID.BG/BG. Cell Immunol 1990;130:106–17.
26. Ali S, El-Rayes BF, Aranha O, Sarkar FH, Philip PA. Sequence dependent potentiation of gemcitabine by flavopiridol in human breast cancer cells. Breast Cancer Res Treat 2005;90:25–31.
27. Jaschke B, Milz S, Vogeser M, et al. Local cyclin-dependent kinase inhibition by flavopiridol inhibits coronary artery smooth muscle cell proliferation and migration: Implications for the applicability on drug-eluting stents to prevent neointima formation following vascular injury. FASEB J 2004;18:1285–7.
28. Rosato RR, Almenara JA, Yu C, Grant S. Evidence of a functional role for p21WAF1/CIP1 down-regulation in synergistic antileukemic interactions between the histone deacetylase inhibitor sodium butyrate and flavopiridol. Mol Pharmacol 2004;65:571–81.
29. Dai Y, Rahmani M, Grant S. Proteasome inhibitors potentiate leukemic cell apoptosis induced by the cyclin-dependent kinase inhibitor flavopiridol through a SAPK/JNK- and NF-κB-dependent process. Oncogene 2003;22:7108–22.
30. Gao N, Dai Y, Rahmani M, Dent P, Grant S. Contribution of disruption of the nuclear factor-κB pathway to induction of apoptosis in human leukemia cells by histone deacetylase inhibitors and flavopiridol. Mol Pharmacol 2004;66:956–63.
31. Jung C, Motwani M, Kortmansky J, et al. The

cyclin-dependent kinase inhibitor flavopiridol potentiates gamma-irradiation-induced apoptosis in colon and gastric cancer cells. Clin Cancer Res 2003;9:6052–61.

32. Nguyen DM, Schrump WD, Chen GA, et al. Abrogation of p21 expression by flavopiridol enhances depsipeptide-mediated apoptosis in malignant pleural mesothelioma cells. Clin Cancer Res 2004;10:1813–25.

33. Shah MA, Kortmansky J, Motwani M, et al. A phase I clinical trial of the sequential combination of irinotecan followed by flavopiridol. Clin Cancer Res 2005;11:3836–45.

34. Gansler T, Gerald W, Anderson G, et al. Characterization of a cell line derived from rhabdoid tumor of kidney. Hum Pathol 1991;22:259–66.

35. Rousseau-Merck MF, Mercier F, Bataille D, Nezelof C. Ectopic G-29 and G-37 glucagon secretion by hypercalcemic infantile renal tumors. Peptides 1986;7 Suppl 1:249–52.

36. Arguello F, Alexander M, Sterry JA, et al. Flavopiridol induces apoptosis of normal lymphoid cells, causes immunosuppression, and has potent antitumor activity *in vivo* against human leukemia and lymphoma xenografts. Blood 1998;91:2482–90.

37. Zhai S, Sausville EA, Senderowicz AM, et al. Clinical pharmacology and pharmacogenetics of flavopiridol 1-h i.v. infusion in patients with refractory neoplasms. Anticancer Drugs 2003;14:125–35.

38. Whitlock JA, Krailo M, Reid JM, et al. Phase I clinical and pharmacokinetic study of flavopiridol in children with refractory solid tumors: a Children's Oncology Group Study. J Clin Oncol 2005;23:9179–86.

Clinical Cancer Research

Rhabdoid Tumor Growth is Inhibited by Flavopiridol

Melissa E. Smith, Velasco Cimica, Srinivasa Chinni, et al.

Clin Cancer Res 2008;14:523-532.